J Surfact Deterg (2016) 19:681–691
DOI 10.1007/s11743-016-1830-y

ORIGINAL ARTICLE

A Comprehensive Study on the Synthesis and Micellization of Disymmetric Gemini Imidazolium Surfactants

Xiaohui Zhao[1] · Dong An[1] · Zhiwen Ye[1]

Received: 7 January 2016 / Accepted: 26 April 2016 / Published online: 23 May 2016

Abstract Two groups of disymmetric Gemini imidazolium surfactants, $[C_{14}C_4C_m\text{im}]Br_2$ ($m = 10$, 12, 14) and $[C_mC_4C_n\text{im}]Br_2$ ($m + n = 24$, $m = 12$, 14, 16, 18) surfactants, were synthesized and their structures were confirmed by ^{1}H NMR and ESI–MS spectroscopy. Their adsorption at the air/water interface, thermodynamic parameters and aggregation behavior were explored by means of surface tension, electrical conductivity and steady-state fluorescence. A series of surface activity parameters, including cmc, γ_{cmc}, π_{cmc}, pC_{20}, cmc/C_{20}, Γ_{max} and A_{min}, were obtained from surface tension measurements. The results revealed that the overall hydrophobic chain length (N_c) for $[C_{14}C_4C_m\text{im}]Br_2$ and the disymmetry (m/n) for $[C_mC_4C_n\text{im}]Br_2$ had a significant effect on the surface activity. The cmc values decreased with an increase of N_c or m/n. The thermodynamic parameters of micellization (ΔG^θ_m, ΔH^θ_m, ΔS^θ_m) derived from the electrical conductivity indicated that the micellization process of $[C_{14}C_4C_m\text{im}]Br_2$ and $[C_mC_4C_n\text{im}]Br_2$ was entropy-driven at different temperatures, but the contribution of ΔH^θ_m to ΔG^θ_m was enhanced by increasing N_c or m/n. The micropolarity and micellar aggregation number (N_{agg}) were estimated by steady-state fluorescence measurements. The results showed that the surfactant with higher N_c or m/n can form larger micelles, due to a tighter micellar structure.

✉ Zhiwen Ye
yezw@mail.njust.edu.cn

[1] School of Chemical Engineering, Nanjing University of Science and Technology, Nanjing 210094, People's Republic of China

Keywords Disymmetric Gemini imidazolium surfactants · Synthesis · Surface activity · Thermodynamic parameters · Micropolarity · Aggregation number

Introduction

Gemini surfactants, "dimers" of single-tailed surfactants linked at the level of, or very close to, the head groups by a spacer group, have gained much attention in the past few decades [1–4]. Compared to the conventional single-tailed surfactants, Gemini surfactants exhibit overwhelming superiority, such as lower critical micelle concentration (cmc), higher adsorption efficiency, better wetting, foaming and lime-soap dispersing properties, and unusual rheological and aggregation properties [5–7], which makes them widely useful in skin care, petrochemistry, medicine, life science, and construction of porous materials [8–13]. Considerable effort has been exercised to design and develop a library of Gemini surfactants with diverse structure and functionality. The most investigated Gemini surfactants are the dicationic quaternary ammonium compounds with the general structure $[C_mH_{2m+1}(CH_3)_2N(CH_2)_sN(CH_3)_2C_nH_{2n+1}]Br_2$, abbreviated as $C_mC_sC_nBr_2$ ($m = n$) [14, 15]. The effect of alkyl tail length and spacer group length on the surface properties and micellization process has been systematically studied. Heterocycles headgroup-based Gemini surfactants, such as pyrrolidinium, imidazolium and hexahydropyridine Gemini surfactants, have also attracted increasing interest, and different hydrophilic head groups have a significant effect on the surface adsorption and aggregation behavior of Gemini surfactants [16–21]. For example, Gemini imidazolium surfactants ($[C_mC_sC_n\text{im}]Br_2$, $m = n$), employing heterocyclic imidazole as the headgroup and methylene as

the spacer group, demonstrate higher surface activity and lower cmc [22–24]. In addition, owing to the existence of imidazolium headgroup, as cationic micelle systems, they show a distinctly greater tendency to self-aggregation and thus are used as supramolecular templates in the preparation of functional materials [25]; as cationic reverse-micelle systems, they display greater solubilization ability compared with cationic Gemini ammonium surfactants [26]. They can form tighter membranes [27] and thus be applied widely in the field of biology due to the strong attraction between the imidazolium headgroup and aromatic rings through π–π interaction [28].

The disymmetric Gemini surfactants consist of two different hydrophobic chains or two different hydrophilic head groups, connected by a rigid or flexible spacer group. Owing to more controlled molecular structures, these surfactants have many peculiar properties, such as the enhanced contribution of enthalpy to the Gibbs free energy [29], higher efficiency of reducing surface tension and greater ability to the formation of micelles caused by the disymmetric Gemini surfactants with ionic–nonionic head groups [30], counterions-free systems constructed by the disymmetric Gemini surfactants containing cationic–anionic head groups [31], and various morphologies of aggregates formed by the dissymmetric Gemini surfactants making use of their different length alkyl chains [32, 33]. Currently, the synthesis and properties of the dissymmetric ammonium Gemini surfactants ($C_mC_sC_nBr_2$, $m \neq n$) [34, 35] and the disymmetric pyrrolidinium Gemini surfactants ($C_mC_sC_nPB$, $m \neq n$) have been researched in detail [36]. Their results indicate the disymmetric degree of the hydrophobic chains have a strong influence on the physicochemical properties of the surfactants. However, no works have focused on preparing and exploring the disymmetric Gemini imidazolium surfactants ($[C_mC_sC_n\text{-im}]Br_2$, $m \neq n$). The motivation of the present work is to further study the effect of disymmetric degree on the physicochemical properties of these surfactants and build up the structure–property relationships of them. Therefore, a series of disymmetric Gemini imidazolium surfactants with a four-methylene spacer group were synthesized and characterized by ^{1}H NMR and ESI–MS spectroscopy (Scheme 1). The investigated surfactants can be divided into two groups: the disymmetric $[C_{14}C_4C_m\text{im}]Br_2$ ($m = 10, 12, 14$) surfactants with 14 carbon atoms in one hydrocarbon chain, and the disymmetric $[C_mC_4C_n\text{im}]Br_2$ ($m + n = 24$, $m = 12, 14, 16, 18$) surfactants with the same total carbon number of 24 in the two hydrophobic chains. Their surface activity, aggregation number and thermodynamic properties of micellization were obtained by means of surface tension, steady-state fluorescence and electrical conductivity measurements. Therefore, the effect of dissymmetry of the hydrophobic chains on the surface activity and micellization process can be discussed comparatively and systematically.

Experimental Section

Materials

Imidazole, potassium hydroxide, dimethyl sulfoxide (DMSO), chloroform, anhydrous magnesium sulfate, ethyl acetate, acetone, hexane, methanol, and isopropanol were purchased from Chengdu Kelong Reagent. Alkyl bromide ($C_nH_{2n+1}Br$, $n = 6, 8, 10, 12, 14, 16$ and 18), 1, 4-dibromobutane, and pyrene (99 %) were purchased from Aladdin Reagent. Benzophenone (C.P.) was purchased from Sinopharm Reagent. Ultrapure water was utilized for preparing all the surfactant solutions.

Synthesis of *N*-Alkyl Imidazole

A mixture of imidazole (30 mmol, 2.04 g), potassium hydroxide (30 mmol, 1.68 g) and dimethyl sulfoxide (10 mL) was stirred for 2 h at room temperature. After that, alkyl bromide (25.0 mmol of 1-bromohexane, 1-bromooctane, 1-bromodecane, 1-bromododecane, 1-bromotetradecane, 1-bromohexadecane, or 1-bromooctadecane) was dropped in slowly and the mixture was stirred for an additional 4 h. Upon completion, water (30 mL) was added to the resulting mixture followed by extraction with chloroform (5 × 30 mL). The combined organic layer was dried over anhydrous magnesium sulfate and the filtrate was concentrated under reduced pressure. The residue was subjected to flash chromatography with ethyl acetate as eluent to give *N*-alkyl imidazole. The respective yields of *N*-hexyl imidazole, *N*-octyl imidazole, *N*-decyl imidazole, *N*-dodecyl imidazole, *N*-tetradecyl imidazole, *N*-hexadecyl imidazole and *N*-octadecyl imidazole are 84.6, 82.3, 81.2, 80.5, 80.4, 79.8 and 79.6 %. ^{1}H NMR (Bruker Avance III 500, 500 MHz, $CDCl_3$) *N*-hexyl imidazole: δ 7.42 (s, –NC*H*N–), 7.01 (s, –NC*H*CHN–), 6.87 (s, –NCHC*H*N–), 3.88 (t, –NCH_2–), 1.73 (m, –NCH$_2$CH_2–), 1.25–1.27 (m, –NCH$_2$CH$_2$(CH_2)$_3$–), 0.85 (t, –CH$_2$CH_3). *N*-octyl imidazole: δ 7.44 (s, –NC*H*N–), 7.03 (s, –NC*H*CHN–), 6.88 (s, –NCHC*H*N–), 3.90 (t, –NCH_2–), 1.75 (m, –NCH$_2$CH_2–), 1.24–1.27 (m, –NCH$_2$CH$_2$(CH_2)$_5$–), 0.85 (t, –CH$_2$CH_3); *N*-decyl imidazole: δ 7.41 (s, –NC*H*N–), 6.99 (s, –NC*H*CHN–), 6.86 (s, –NCHC*H*N–), 3.88 (t, –NCH_2–), 1.74 (m, –NCH$_2$CH_2–), 1.21–1.25 (m, –NCH$_2$CH$_2$(CH_2)$_7$–), 0.85 (t, –CH$_2$CH_3); *N*-dodecyl imidazole: δ 7.44 (s, –NC*H*N–), 7.03 (s, –NC*H*CHN–), 6.88 (s, –NCHC*H*N–), 3.90 (t, –NCH_2–), 1.75 (m, –NCH$_2$CH_2–), 1.23−1.27 (m, –NCH$_2$CH$_2$(CH_2)$_9$–), 0.88 (t, –CH$_2$CH_3); *N*-tetradecyl imidazole: δ 7.43 (s, –NC*H*N–), 7.01 (s, –NC*H*CHN–), 6.88 (s,

Scheme 1 Synthesis route of the disymmetric Gemini imidazolium surfactants

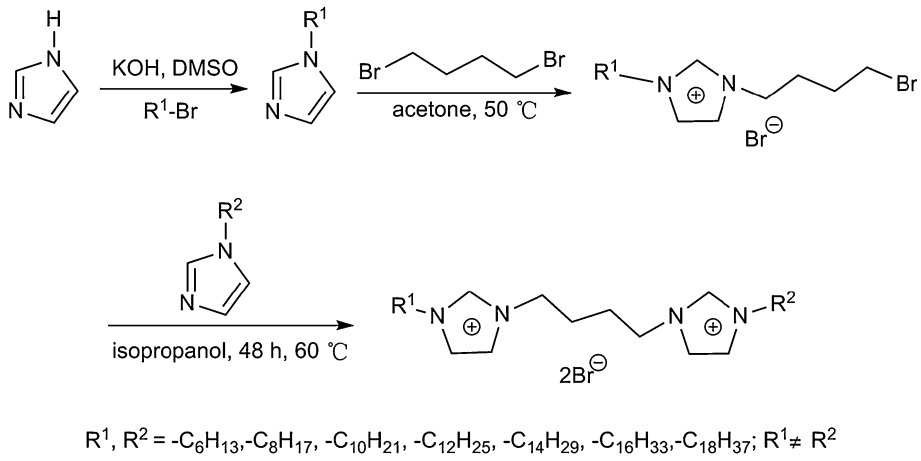

R^1, R^2 = -C_6H_{13},-C_8H_{17}, -$C_{10}H_{21}$, -$C_{12}H_{25}$, -$C_{14}H_{29}$, -$C_{16}H_{33}$,-$C_{18}H_{37}$; $R^1 \neq R^2$

–NCH*CH*N–), 3.89 (t, –N*CH*$_2$–), 1.75 (m, –NCH$_2$*CH*$_2$–), 1.22–1.26 (m, –NCH$_2$CH$_2$*(CH$_2$)$_{11}$*–), 0.85 (t, –CH$_2$*CH*$_3$); *N*-hexadecyl imidazole: δ 7.45 (s, –N*CH*N–), 7.05 (s, –N*CH*CHN–), 6.90 (s, –NCH*CH*N–), 3.91 (t, –N*CH*$_2$–), 1.76 (m, –NCH$_2$*CH*$_2$–), 1.25–1.32 (m, –NCH$_2$CH$_2$*(CH$_2$)$_{13}$*–), 0.87 (t, –CH$_2$*CH*$_3$); *N*-octadecyl imidazole: δ 7.44 (s, –N*CH*N–), 7.04 (s, –N*CH*CHN–), 6.89 (s, –NCH*CH*N–), 3.91 (t, –N*CH*$_2$–), 1.76 (m, –NCH$_2$*CH*$_2$–), 1.21–1.30 (m, –NCH$_2$CH$_2$*(CH$_2$)$_{15}$*–), 0.87 (t, –CH$_2$*CH*$_3$).

Synthesis of 1-(4-Bromobutyl)-3-Alkylimidazolium Bromide

1,4-dibromobutane (36.0 mmol, 7.70 g) was dissolved in dry acetone (50 mL) and the obtained *N*-alkyl imidazole (9.0 mmol of *N*-hexyl imidazole, *N*-octyl imidazole, *N*-decyl imidazole, or *N*-dodecyl imidazole) was added gradually. The reaction mixture was refluxed at 50 °C under nitrogen atmosphere and the reaction was monitored by TLC analysis. After the reaction finished, the solvent was removed under reduced pressure, and subsequently the un-reacted 1, 4-dibromobutane was washed thoroughly with hexane. The collected viscous liquid was purified by silica column chromatography with mixtures of acetone/methanol (10:1, by vol) as eluent to afford 1-(4-bromobutyl)-3-alkylimidazolium bromide. The yields of 1-(4-bromobutyl)-3-hexylimidazolium bromide, 1-(4-bromobutyl)-3-octylimidazolium bromide, 1-(4-bromobutyl)-3-decylimidazolium bromide and 1-(4-bromobutyl)-3-dodecylimidazolium bromide are 72.5, 74.1, 76.8 and 80.3 %, respectively. ^{1}H NMR (500 MHz, $CDCl_3$) 1-(4-bromobutyl)-3-hexylimidazolium bromide: δ 10.32 (s, –N*CH*N–), 7.68 (s, –N*CH*CHN–), 7.45 (s, –NCH*CH*N–), 4.43 (t, –N$^+$–*CH*$_2$–), 4.25 (t, –N*CH*$_2$–), 3.41 (t, –*CH*$_2$Br), 2.01–2.09 (m, –N$^+$–CH$_2$*CH*$_2$–), 1.79–1.94 (m, –NCH$_2$*(CH$_2$)$_2$*–), 1.21 (m, –N$^+$–CH$_2$CH$_2$*(CH$_2$)$_3$*–), 0.79 (t, –CH$_2$*CH*$_3$); 1-(4-bromobutyl)-3-octylimidazolium bromide: δ 10.39 (s, –N*CH*N–), 7.63 (s, –N*CH*CHN–), 7.40 (s, –NCH*CH*N–), 4.47 (t, –N$^+$–*CH*$_2$–), 4.28 (t, –N*CH*$_2$–), 3.45 (t, –*CH*$_2$Br), 2.06–2.14 (m, –N$^+$–CH$_2$*CH*$_2$–), 1.90 (m, –NCH$_2$*(CH$_2$)$_2$*–), 1.24 (m, –N$^+$–CH$_2$CH$_2$*(CH$_2$)$_5$*), 0.82 (t, –CH$_2$*CH*$_3$); 1-(4-bromobutyl)-3-decylimidazolium bromide: δ 10.31 (s, –N*CH*N–), 7.70 (s, –N*CH*CHN–), 7.46 (s, –NCH*CH*N–), 4.45 (t, –N$^+$–*CH*$_2$–), 4.29 (t, –N*CH*$_2$–), 3.43 (t, –*CH*$_2$Br), 2.08 (m, –N$^+$–CH$_2$*CH*$_2$–), 1.92 (m, –NCH$_2$*(CH$_2$)$_2$*–), 1.26 (m, –N$^+$–CH$_2$CH$_2$*(CH$_2$)$_7$*–), 0.85 (t, –CH$_2$*CH*$_3$); 1-(4-bromobutyl)-3-dodecylimidazolium bromide: δ 10.49 (s, –N*CH*N–), 7.62 (s, –N*CH*CHN–), 7.40 (s, –NCH*CH*N–), 4.48 (t, –N$^+$–*CH*$_2$–), 4.28 (t, –N*CH*$_2$–), 3.45 (t, –*CH*$_2$Br), 2.11 (m, –N$^+$–CH$_2$*CH*$_2$–), 1.91 (m, –NCH$_2$*(CH$_2$)$_2$*–), 1.17–1.33 (m, –N$^+$–CH$_2$CH$_2$*(CH$_2$)$_9$*–), 0.84 (t, –CH$_2$*CH*$_3$).

Synthesis of the Disymmetric Gemini Imidazolium Surfactants

An amount of 5.0 mmol of the obtained 1-(4-bromobutyl)-3-alkylimidazolium bromide (in which the alkyl were hexyl, octyl, decyl, or dodecyl, respectively) was dissolved in isopropanol (20 mL), followed by addition of 7.5 mmol of *N*-alkyl imidazole (in which the alkyl were octadecyl, hexadecyl, tetradecyl, or tetradecyl, correspondingly). The mixture was stirred at 60 °C for 48 h under nitrogen atmosphere. After removal of isopropanol, the residue was washed with ethyl acetate, purified three times by recrystallization in acetone and then dried under vacuum for 48 h, to yield the disymmetric Gemini imidazolium surfactants as white powders. The respective yields of [C_{18}-C_4C_6im]Br_2, [$C_{16}C_4C_8$im]Br_2, [C_{14} C_4C_{10}im]Br_2 and [$C_{14}C_4C_{12}$im]Br_2 are 85.5, 87.3, 88.2 and 89.0 %. ^{1}H NMR (500 MHz, $CDCl_3$) Take [$C_{14}C_4C_{10}$im]Br_2 as an example: δ 10.27 (s, 2H, –N*CH*N–), 7.96 (s, 2H, –N*CH*CHN–), 7.15 (s, 2H, –NCH*CH*N–), 4.58 (t, 4H, –N$^+$–*CH*$_2$–), 4.24 (t, 4H, –N*CH*$_2$–), 2.22 (m, 4H, –N$^+$–CH$_2$*CH*$_2$–), 1.90 (m, 4H,

–NCH_2CH_2–), 1.19–1.37 (m, 36H, –N^+–$CH_2CH_2CH_2$–), 0.87 (t, 6H, –CH_2CH_3); MS (Finnigan TSQ Quantum ultra AM, ESI) $[M–2Br]^{2+:}$ 264.32. $[C_{14}C_4C_{12}im]Br_2$: δ 10.31 (s, 2H, –NCHN–), 7.98 (s, 2H, –NCHCHN–), 7.15 (s, 2H, –NCHCHN–), 4.58 (t, 4H, –N^+–CH_2–), 4.24 (t, 4H, –NCH_2–), 2.23 (m, 4H, –N^+–CH_2CH_2–), 1.89 (m, 4H, –NCH_2CH_2–), 1.21–1.36 (m, 40H, –N^+–$CH_2CH_2CH_2$–), 0.87 (t, 6H, –CH_2CH_3); MS (ESI) $[M-2Br]^{2+:}$ 278.30.

Synthesis of the Symmetric Gemini Imidazolium Surfactants ($[C_mC_4C_mim]Br_2$, $m = 12, 14$)

A mixture of 10 mmol of *N*-dodecyl imidazole or *N*-tetradecyl imidazole, 1,4-dibromobutane (4 mmol, 0.856 g) and isopropanol (20 mL) was stirred for 48 h at 60 °C under nitrogen atmosphere. After removal of isopropanol, the residue was washed with ethyl acetate, further purified four times by recrystallization in acetone and then dried under vacuum for 48 h. $[C_{12}C_4C_{12}im]Br_2$ and $[C_{14}\ C_4C_{14}im]Br_2$ as the white powder were gained. The respective yields of $[C_{12}C_4C_{12}im]Br_2$ and $[C_{14}\ C_4C_{14}im]Br_2$ are 92.4 % and 93.3 %. ^{1}H NMR (500 MHz, $CDCl_3$) $[C_{12}C_4C_{12}im]Br_2$: δ 10.19 (s, 2H, –NCHN–), 8.05 (s, 2H, –NCHCHN–), 7.21 (s, 2H, –NCHCHN–), 4.58 (t, 4H, –N^+–CH_2–), 4.24 (t, 4H, –NCH_2–), 2.19 (m, 4H, –N^+–CH_2CH_2–), 1.88 (m, 4H, –NCH_2CH_2–), 1.20–1.35 (m, 36H, –N^+–$CH_2CH_2(CH_2)_9$–), 0.86 (t, 6H, –CH_2CH_3); MS (ESI) $[M-2Br]^{2+:}$ 264.27. $[C_{14}C_4\ C_{14}im]Br_2$ δ 10.30 (s, 2H, –NCHN–), 7.99 (s, 2H, –NCHCHN–), 7.16 (s, 2H, –NCHCHN–), 4.58 (t, 4H, –N^+–CH_2–), 4.24 (t, 4H, –NCH_2–), 2.22 (m, 4H, –N^+–CH_2CH_2–), 1.89 (m, 4H, –NCH_2CH_2–), 1.20–1.37 (m, 44H, –N^+–$CH_2CH_2(CH_2)_{11}$–), 0.87 (t, 6H, –CH_2CH_3); MS (ESI) $[M-2Br]^{2+:}$ 292.32.

The Krafft temperatures of $[C_mC_4C_n]Br_2$ ($m + n = 24$, $m = 12, 14, 16, 18$) were all lower than 15 °C. For $[C_{14}C_4C_{12}im]Br_2$ and $[C_{14}C_4C_{14}im]Br_2$, their solubility was not better than those of $[C_mC_4C_n]Br_2$ ($m + n = 24$, $m = 12, 14, 16, 18$), but when their concentration was not higher than 2 mmol/L, they can still remain as a clear aqueous solution at 15 °C. Therefore, in our experimental range of the prepared surfactant concentration, all the experiments can be performed at or above 15 °C.

Equilibrium Surface Tension Measurements

The equilibrium surface tension was estimated by using the pendant drop method, performed on an optical contact angle measuring instrument (OCA 40; Beijing Eastern Dataphy Instruments). All measurements were taken at 25.0 ± 0.1 °C and the surfactant solutions were kept still for 30 min in order to achieve the system equilibrium.

Electrical Conductivity Measurements

The electrical conductivity of surfactant solutions at five different temperatures was obtained by a conductivity analyzer (DDS-11A; Shanghai Leici TRONY Instrument). The measurements were repeated three times for each temperature and each temperature was controlled with a precision of ±0.1 °C.

Steady-State Fluorescence Measurements

Fluorescence spectra were recorded on a FluoroMax-4 spectrofluorometer with a 1-cm^2 quartz cuvette. Pyrene was used as the fluorescence probe and benzophenone as the quencher. The concentration of pyrene was kept at 1.0×10^{-6} mol L^{-1}. The excitation wavelength was fixed at 335 nm and the emission spectra range was selected from 350 to 500 nm. The slit widths of excitation and emission were set at 8 and 2 nm, respectively.

Results and Discussion

Adsorption at Air/Water Interface

The adsorption at air/water interface for Gemini imidazolium surfactants, including $[C_{12}C_4C_{12}im]Br_2$, $[C_{14}C_4C_{10}im]Br_2$, $[C_{16}C_4C_8im]Br_2$, $[C_{18}C_4C_6im]Br_2$, $[C_{14}C_4C_{12}im]Br_2$ and $[C_{14}C_4C_{14}im]Br_2$, was evaluated by the equilibrium surface tension as a function of surfactant concentration (Fig. 1). The surface tension gradually decreased with the increase of surfactant concentration and then reached a plateau. The concentration of the clear

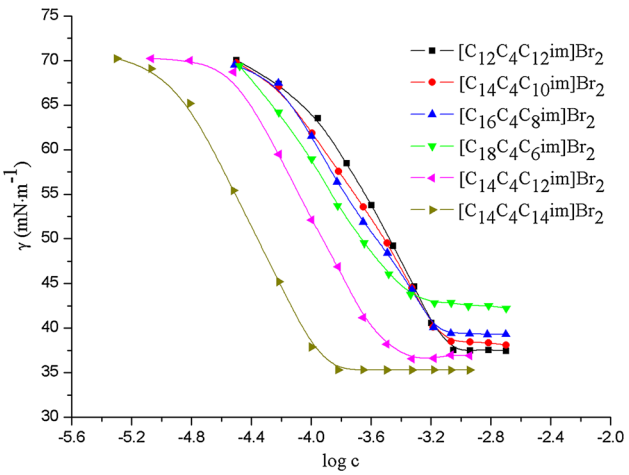

Fig. 1 Plots of surface tension vs. log *c* at 25 °C for the disymmetric Gemini imidazolium surfactants in aqueous solution. The error of surface tension value is ±0.2 mN/m

Table 1 Surface activity of the disymmetric Gemini imidazolium surfactants at 25 °C

Surfactant	*m/n*	cmc (mmol/L)			γ_{cmc} (mN/m)	π_{cmc} (mN/m)	pC_{20}	cmc/C_{20}	Γ_{max} (μmol/m^2)	A_{min} (nm^2)	N_{agg}
		Surface tension	Electrical conductivity	Steady-state fluorescence							
$[C_{12}C_4C_{12}im]Br_2$	1	0.73	0.738	0.73	37.50	34.47	3.54	2.50	1.76	0.94	16
$[C_{14}C_4C_{10}im]Br_2$	1.4	0.69	0.717	0.70	38.34	33.63	3.59	2.68	1.56	1.06	18
$[C_{16}C_4C_8im]Br_2$	2	0.63	0.649	0.64	39.36	32.61	3.65	2.81	1.49	1.11	21
$[C_{18}C_4C_6im]Br_2$	3	0.50	0.565	0.55	42.59	29.38	3.76	2.88	1.29	1.29	27
$[C_{14}C_4C_{12}im]Br_2$	1.17	0.26	0.316	0.29	36.77	35.20	4.02	2.72	1.88	0.88	20
$[C_{14}C_4C_{14}im]Br_2$	1	0.12	0.132	0.13	35.31	36.66	4.42	3.16	1.96	0.85	22

breakpoint in the γ-log c curves corresponded to the critical micelle concentration (cmc), indicating the formation of micelles, and the surface tension at the cmc was defined as γ_{cmc}. In addition, the absence of a minimum near the breakpoint suggested a low concentration of surface chemical impurities for the investigated Gemini surfactants [20]. In this work, the classic Gibbs adsorption theory was used to study the surface properties of the disymmetric Gemini imidazolium surfactants.

The maximum surface excess concentration, Γ_{max}, and the minimum average area occupied by a single surfactant molecule at the air/water interface, A_{min}, can be estimated according to the Gibbs adsorption equation [37]:

$$\Gamma_{max} = -\frac{1}{2.303nRT} \times \frac{d\gamma}{d\log c} \quad (1)$$

$$A_{min} = \frac{10^{24}}{N_A \Gamma_{max}} \quad (2)$$

where Γ_{max} is in μmol/m^2, R is the gas constant (8.314 J mol^{-1} K^{-1}), T is the absolute temperature in Kelvin, γ is the surface tension in mN m^{-1}, c is the surfactant concentration and ($d\ \gamma/d$ log$c$) is the slope of the linear part in the γ-log c curves where the surfactant concentration is below the cmc. In aqueous solutions of the investigated Gemini imidazolium surfactants, n is taken as 3, considering one dimeric ion and two counterions in the surfactant molecule [38]. N_A is Avogadro's number and A_{min} is in nm^2/molecule.

The adsorption efficiency at the air–water interface, pC_{20}, and the surface pressure at cmc, π_{cmc}, are obtained from Eqs. (3, 4):

$$pC_{20} = -\log C_{20} \quad (3)$$

$$\pi_{cmc} = \gamma_0 - \gamma_{cmc} \quad (4)$$

where C_{20} represents the surfactant concentration at which the surface tension of water is reduced by 20 mN·m^{-1}. Generally, the larger the value of pC_{20}, the higher the adsorption efficiency of the surfactant.

γ_0 is the surface tension of water and γ_{cmc} is the surface tension of surfactant solution at the cmc. The larger the value of π_{cmc}, the higher the effectiveness of the surfactant to lower the surface tension of water. The value of cmc/C_{20} is related with the structural factors in the adsorption and micellization process. The surfactant with larger cmc/C_{20} value a tends more to adsorb at the interface than to form micelles. Based on the γ-log c curves, the above-described physicochemical parameters for $[C_{14}C_4C_m im]Br_2$ and $[C_mC_4C_n im]Br_2$, such as cmc, γ_{cmc}, π_{cmc}, pC_{20}, cmc/C_{20}, Γ_{max} and A_{min}, are listed in Table 1.

From Fig. 2a, the values of cmc for the disymmetric $[C_{14}C_4C_m im]Br_2$ series decreased with the increasing total carbon number in two hydrocarbon chains regardless of the degree of disymmetry, implying that the longer overall hydrophobic chain length (N_c), the higher the aggregation abilityas. The contribution of each additional methylene unit to the cmc values of $[C_{14}C_4C_m im]Br_2$ was higher than that of classic single-tailed surfactant homologues [C_n mim]Br [39, 40]. It can be noticed that the γ_{cmc} values of $[C_{14}C_4C_m im]Br_2$ decreased with the increasing N_c, indicating that $[C_{14}C_4C_{14}im]Br_2$ possessed higher surface activity, which could also be found from the changes of π_{cmc} and pC_{20} values. For the disymmetric $[C_{14}C_4C_m im]Br_2$ series, the changes of cmc, γ_{cmc}, π_{cmc} and pC_{20} values with N_c were similar to those of the disymmetric Gemini pyrrolidinium surfactants ($C_mC_3C_{14}$-PB, m = 10, 12, 14) [36]. The cmc/C_{20} values increased with the increase of N_c, which suggested that, in comparison with micellization process, the adsorption at the air/water interface for $[C_{14}C_4C_m im]Br_2$ with longer hydrophobic chains was much easier. However, the A_{min} values of $[C_{14}C_4C_m im]Br_2$ decreased with the increasing N_c, meaning that $[C_{14}C_4C_{14}im]Br_2$ had a higher packing density. The hydrophobic interactions were strengthened with the increasing N_c, which could promote the surfactant molecules to pack much more densely, and consequently the A_{min} values will decrease. This result was different from $C_mC_3C_{14}$PB, and the possible reason was

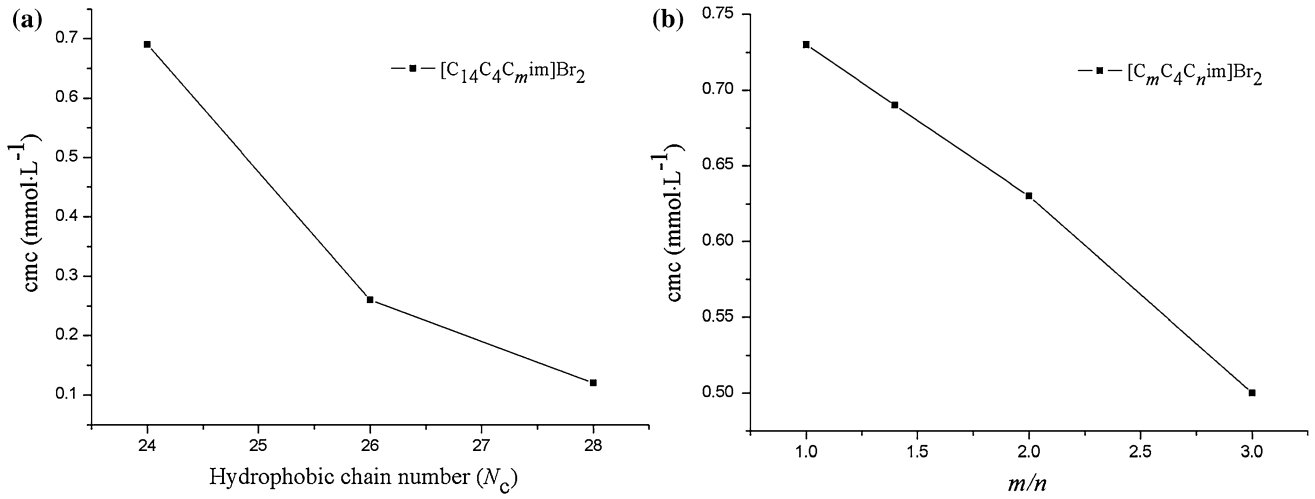

Fig. 2 Effect of the overall hydrophobic chain length (**a**) and the disymmetry (**b**) on cmc

that the longer hydrophobic chains were more prone to bending.

The typical effect of the disymmetry on the cmc can be found from the disymmetric [$C_mC_4C_n$im]Br_2 series (Fig. 2b), those surfactants with the same total carbon number of 24 in two hydrocarbon chains. Higher structural disymmetry resulted in a lower cmc by employing *m/n* as the degree of disymmetry and a similar conclusion was also observed in other disymmetric Gemini surfactants [29, 34, 36]. Clearly, the introduction of disymmetry to the hydrophobic chains can strengthen the aggregation behavior, and adding two methylene groups to one longer chain was more efficient in lowering the cmc than adding each of them to two chains separately. The hydrophobic interactions had two contributions to the aggregation behavior, intermolecular and intramolecular. The latter will be weaker because the spacer groups kept the two hydrophobic chains apart. For the symmetric Gemini surfactants, the hydrophobic interactions will be minimized due to the equal number of hydrophobic units for both intramolecular and intermolecular interactions. However, for the disymmetric Gemini surfactants, as *m/n* increased, the ratio of hydrophobic units interacting intermolecularly to those intramolecularly will increase [41]. Therefore, the overall hydrophobic interactions were gradually improved with the increasing *m/n*, which made a positive contribution to the formation of micelles. On the other hand, both the γ_{cmc} and A_{min} values increased with the increase of *m/n*, implying that the Gemini surfactants with a higher disymmetry were packed more loosely at the air/water interface. This might be attributed to the fact that the longer hydrocarbon chain for [$C_{18}C_4C_6$im]Br_2 with the highest disymmetry was more prone to bend at the interface, which made the surface area per molecule larger, and therefore resulted in the larger γ_{cmc} value. The γ_{cmc} and A_{min} values showed the opposite relation with the disymmetry in comparison with $C_mC_3C_n$PB ($m + n = 24$, $m = 12$, 14, 16). Furthermore, the increase in cmc/C_{20} indicated that the adsorption at the air/water interface was more favored over the micellization process for those surfactants with the higher disymmetry. The same conclusion could also be speculated from the variation in pC_{20} values.

Degree of Counterion Binding to Micelles

The degree of counterion binding to micelles (β), a fundamental feature of the ionic surfactant micelles, is certain to have an important role in the micellization process and various aggregation behaviors in aqueous solutions. An understanding of β can provide insight into the specific properties of ionic surfactants and a further investigation of new ionic Gemini surfactants. The electrical conductivity measurements are often used to determine the cmc and β values. For each of [$C_{14}C_4C_m$im]Br_2 or [$C_mC_4C_n$im]Br_2 series, Fig. 3 gives the plots of the conductivity (κ) versus surfactant concentration (c) at five different temperatures. It was evident that all plots had breakpoints, and that the concentration corresponded to the cmc. This was a result of the reduction of effective charges in the solution, due to the binding of some counterions to the micelles above the cmc. Moreover, the degree of counterion dissociation (α) can be taken as the ratio of the slopes of two fitted lines above and below the cmc. Thus, the β values could be obtained by using $\beta = 1 - \alpha$. The cmc and β values of [$C_{14}C_4C_m$-im]Br_2 and [$C_mC_4C_n$im]Br_2 series at five different temperatures are listed in Table 2. It can be seen that the cmc

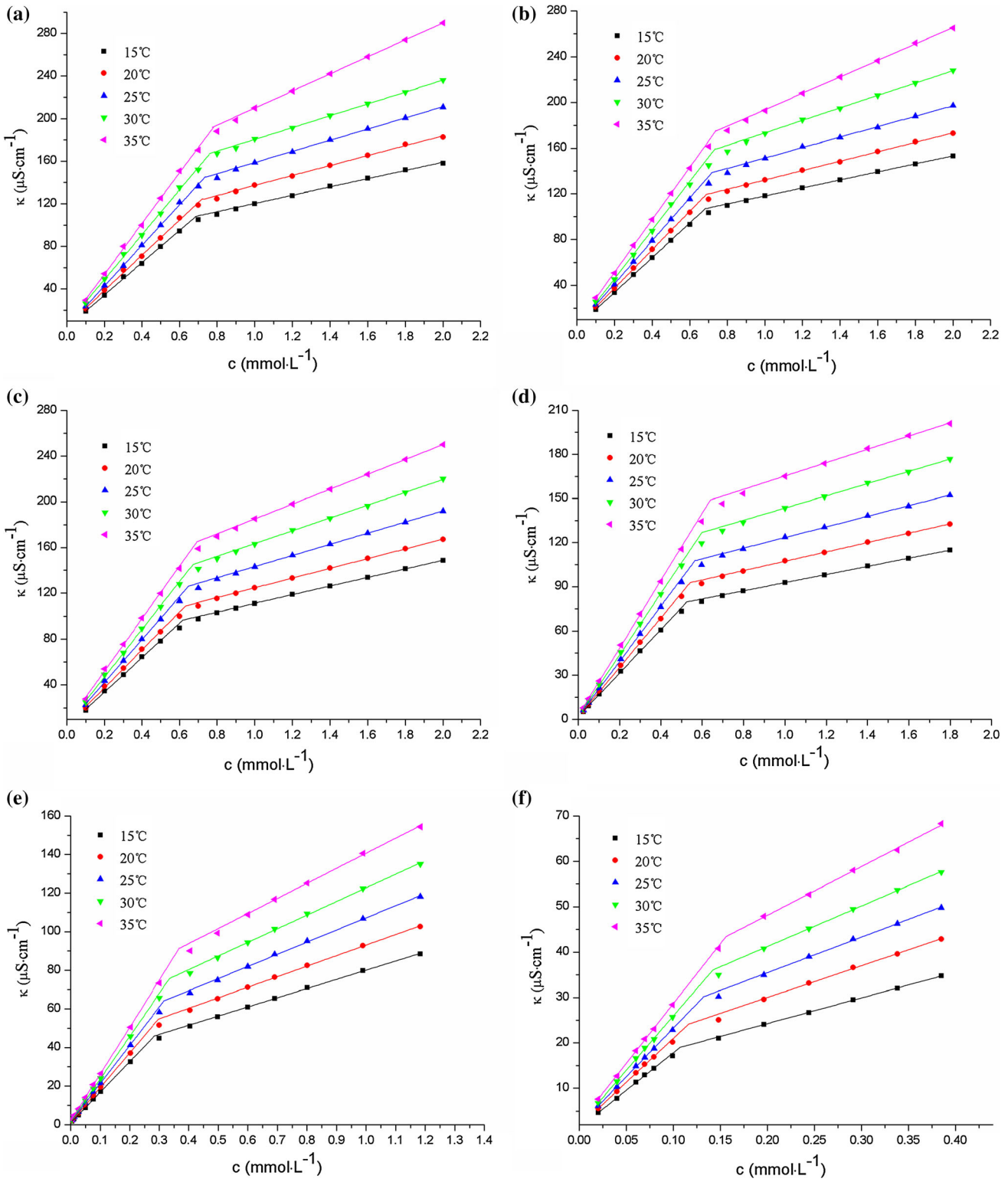

Fig. 3 Plots of electrical conductivity vs. surfactant concentration at five different temperatures. The error of electrical conductivity value is ±0.2 μS/cm. $[C_{12}C_4C_{12}im]Br_2$ (**a**), $[C_{14}C_4C_{10}im]Br_2$ (**b**), $[C_{16}C_4C_8im]Br_2$ (**c**), $[C_{18}C_4C_6im]Br_2$ (**d**), $[C_{14}C_4C_{12}im]Br_2$ (**e**), $[C_{14}C_4C_{14}im]Br_2$ (**f**)

values for all the studied surfactants increased upon raising the temperature, and that the cmc values estimated from the electrical conductivity at 25 °C were in accordance with those obtained from the surface tension. A reasonable explanation was that the ordered water molecules around the hydrophobic chains may be broken at a higher

Table 2 Thermodynamic parameters of micellization for the disymmetric Gemini imidazolium surfactants at different temperatures

Surfactant	*m/n*	Temperature (°C)	cmc (mmol/L)	β	ΔG_m^θ (kJ/mol)	ΔH_m^θ (kJ/mol)	$T\Delta S_m^\theta$ (kJ/mol)
$[C_{12}C_4C_{12}im]Br_2$	1	15	0.706	0.745	−47.12	−5.059	42.06
		20	0.723	0.742	−47.75	−5.227	42.52
		25	0.738	0.730	−48.14	−5.370	42.77
		30	0.758	0.726	−48.72	−5.539	43.18
		35	0.765	0.709	−49.00	−5.667	43.33
$[C_{14}C_4C_{10}im]Br_2$	1.4	15	0.682	0.768	−47.88	−5.858	42.03
		20	0.687	0.757	−48.38	−6.026	42.35
		25	0.717	0.756	−48.99	−6.229	42.76
		30	0.731	0.737	−49.19	−6.370	42.82
		35	0.740	0.715	−49.31	−6.499	42.81
$[C_{16}C_4C_8im]Br_2$	2	15	0.619	0.751	−47.83	−6.769	41.06
		20	0.631	0.743	−48.36	−6.974	41.38
		25	0.649	0.739	−48.95	−7.197	41.75
		30	0.672	0.731	−49.39	−7.406	41.98
		35	0.693	0.716	−49.63	−7.586	42.04
$[C_{18}C_4C_6im]Br_2$	3	15	0.525	0.813	−50.24	−12.52	37.72
		20	0.542	0.810	−50.88	−12.93	37.95
		25	0.565	0.807	−51.48	−13.36	38.13
		30	0.599	0.802	−51.93	−13.77	38.16
		35	0.639	0.800	−52.43	−14.21	38.22
$[C_{14}C_4C_{12}im]Br_2$	1.17	15	0.284	0.700	−49.61	−15.02	34.59
		20	0.297	0.696	−50.17	−15.51	34.66
		25	0.316	0.682	−50.34	−15.91	34.43
		30	0.335	0.680	−50.88	−16.43	34.45
		35	0.367	0.679	−51.30	−16.97	34.33
$[C_{14}C_4C_{14}im]Br_2$	1	15	0.107	0.658	−52.26	−22.20	30.06
		20	0.116	0.638	−52.20	−22.70	29.50
		25	0.132	0.635	−52.47	−23.44	29.03
		30	0.142	0.628	−52.83	−24.13	28.70
		35	0.156	0.593	−52.16	−24.40	27.76

temperature, which would be unfavorable for the formation of micelles [42]. All the values of β showed a monotonous decrease with the increasing temperature, which indicated the decrease of charge density on the micelle surface. The same trends of cmc and β values with temperature have also been observed for the disymmetric Gemini pyrrolidinium surfactants $C_mC_3C_{14}PB$ and $C_mC_3C_nPB$.

Thermodynamics Parameters

The thermodynamic parameters for the micellization process of $[C_{14}C_4C_m im]Br_2$ and $[C_mC_4C_n im]Br_2$ series were investigated by employing the mass action model [43]. The standard Gibbs free energy change (ΔG_m^θ), the standard enthalpy change (ΔH_m^θ), and standard entropy change (ΔS_m^θ) for the micellization process can be determined from Eqs. (5–7):

$$\Delta G_m^\theta = RT(1+\beta)\ln X_{cmc} \tag{5}$$

$$\Delta H_m^\theta = \left[\frac{\partial(\Delta G_m^\theta/T)}{\partial(1/T)}\right]\Delta H_m^\theta = -RT^2(1+\beta)\frac{d\ln(X_{cmc})}{dT} \tag{6}$$

$$\Delta S_m^\theta = \frac{\Delta H_m^\theta - \Delta G_m^\theta}{T} \tag{7}$$

where R is the gas constant (8.314 J mol^{-1} K^{-1}), T is the absolute temperature in K, β is the degree of counterion binding to micelles which was obtained previously, and X_{cmc} is the cmc expressed in mol fractions.

The corresponding thermodynamic parameters of micellization for all the investigated surfactants at five different temperatures are shown in Table 2. The values of ΔG_m^θ are all negative, meaning that the aggregation for each surfactant in aqueous solution is spontaneous. Notably, both the overall hydrophobic chain length and the disymmetry degree greatly

affected the thermodynamic parameters, or, in other words, the micellization process. The observed more negative ΔG_m^θ values for $[C_{14}C_4C_m\text{im}]Br_2$ series with longer overall hydrophobic chains indicated a stronger tendency to micellization due to greater hydrophobic interactions. Although the changes of ΔG_m^θ values for $[C_mC_4C_n\text{im}]Br_2$ series with an increase of the disymmetry were not so large, it demonstrated that the more negative ΔG_m^θ of $[C_{18}C_4C_6\text{im}]Br_2$ with a higher disymmetry was more beneficial to micellization than that of $[C_{12}C_4C_{12}\text{im}]Br_2$. Simultaneously, the values of the standard enthalpy (ΔH_m^θ) for each surfactant were also negative, indicating that the formation process of micelles was exothermic, which can be attributed to possible surfactant–solvent interactions [17]. Additionally, all the ΔH_m^θ values changed little as the temperature increased, suggesting no significant changes in the environment around the hydrophobic chains of surfactant molecule. The data from Table 2 indicated the ΔS_m^θ values were positive in all cases and the values of $T\Delta S_m^\theta$ were much larger than that of $|\Delta H_m^\theta|$. The negative values of ΔG_m^θ were mainly due to the larger positive ΔS_m^θ, implying that the micellization for $[C_{14}C_4C_m\text{im}]Br_2$ or $[C_mC_4C_n\text{im}]Br_2$ series was entropy-driven. It can be concluded that the driving force of micellization process was the tendency of hydrophobic chains to transfer from the solvent to the interior of micelle. In general, there are mainly four contributions to ΔH_m^θ for the Gemini surfactants: the van der Waals interaction between the alkyl chains, the hydrophobic interaction, the head group repulsion and the configuration of spacer chains [44]. Among these interactions, the van der Waals interaction and the hydrophobic interaction will lead to the changes in the ΔH_m^θ values for the present investigated surfactants. As was previously discussed in our work, the hydrophobic interactions increased significantly with increasing N_c and m/n, which made the ΔH_m^θ values more negative. Consequently, the overall hydrocarbon chain length and the degree of disymmetry had a significant effect on the contribution of ΔH_m^θ to ΔG_m^θ. For the $[C_{14}C_4C_m\text{im}]Br_2$ series, the contribution of ΔH_m^θ to ΔG_m^θ increased when the overall hydrocarbon chain length was increased, which was similar to those of the symmetric $[C_mC_4C_m\text{im}]Br_2$ and the disymmetric $C_mC_3C_{14}$-PB. The $|\Delta H_m^\theta|$ values for $[C_{14}C_4C_{14}\text{im}]Br_2$ were nearly equal to the values of $T\Delta S_m^\theta$ with the increase in the temperature. On the other hand, for the $[C_mC_4C_n\text{im}]Br_2$ series, a higher degree of disymmetry can result in a higher contribution of ΔH_m^θ to ΔG_m^θ, being consistent with those of the disymmetric $C_mC_6C_nBr_2$ [34] and the disymmetric $C_mC_3C_n$PB. From the data in Table 2, the changes of ΔH_m^θ values at 25 °C were from −5.370 to −13.36 kJ/mol as the disymmetry increased. The introduction of disymmetry to the hydrophobic chain shed new light on the possibility of adjusting micellization process further.

Micropolarity and Micellar Aggregation Number

It is well known that pyrene is used as a fluorescence probe to investigate the cmc and polarity of the micellar microenvironment. Normally, the fluorescence emission spectra of pyrene have five vibration bands after the excitation at 335 nm. The ratio of fluorescence intensity (I_1/I_3) between the first vibronic band (373 nm) and the third vibronic band (384 nm) is strongly dependent on the position of the pyrene in micelles and thus can be seen as a measure for the polarity of the micellar microenvironment [45]. Once the surfactant molecules begin to form micelles, the extreme hydrophobic pyrene molecules will transfer from the water environment into the interior hydrophobic region, which was reflected as a sharp drop in the I_1/I_3 value. The concentration corresponding to the sharp drop was taken as the cmc. Figure 4 gives the relationship between the I_1/I_3 ratio and the concentration of all the investigated surfactants. For the $[C_{14}C_4C_m\text{im}]Br_2$ or $[C_mC_4C_n\text{im}]Br_2$ series, the values of cmc determined from the fluorescence plots shown in Table 1 were consistent with those estimated by the methods of electrical conductivity and surface tension. The values of I_1/I_3 were independent of the surfactant concentration above cmc and almost the same for the $[C_{14}C_4C_m\text{im}]Br_2$ or $[C_mC_4C_n\text{im}]Br_2$ series, suggesting that the hydrophobic chains length and the disymmetry have little effect on the micropolarity that was sensed by the pyrene. Moreover, the low I_1/I_3 values indicated that the pyrene was solubilized in the palisade layer near the polar head groups [22]. On the one hand, as the N_c or m/n ratio increased, the hydrophobic interaction was gradually optimized. This was expected to result in a decrease of micropolarity, owing to the tighter packing of

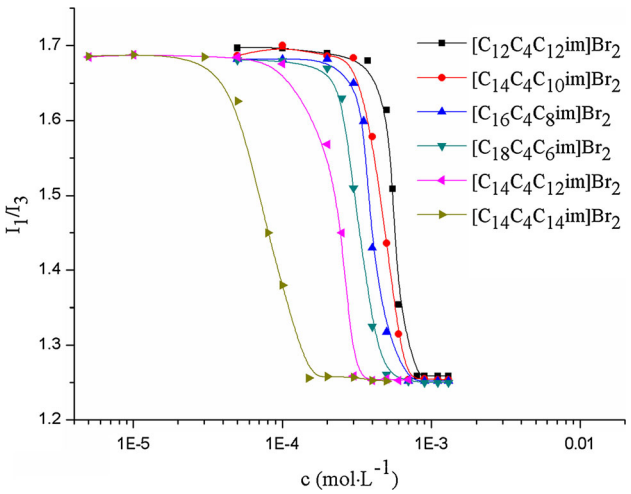

Fig. 4 I_1/I_3 ratio of pyrene as a function of the concentration for the disymmetric Gemini imidazolium surfactants in aqueous solution

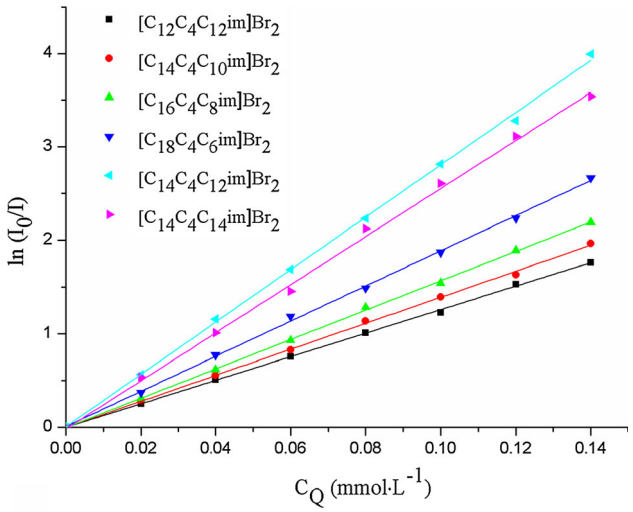

Fig. 5 ln (I_0/I) of pyrene as a function of concentration of the quencher benzophenone in the surfactant aqueous solution

the surfactant alkyl chains. On the other hand, the tighter packing structure may make the pyrene slightly closer to the micellar surface and thus cause an increase of micropolarity, which compensated the first effect just discussed. As a result, the micropolarity of these investigated surfactants micelles that was sensed by the pyrene was observed to be almost the same.

The micellar aggregation number, N_{agg}, was measured by fluorescence quenching experiments [46] and calculated by Eq. (8):

$$\ln\left(\frac{I_0}{I}\right) = \frac{N_{agg}C_Q}{C_S - \text{cmc}} \tag{8}$$

where I_0 and I are the fluorescence intensities of pyrene in the absence and presence of the quencher at a specific wavelength of 373 nm, and C_Q and C_S are the molar concentration of quencher and surfactant, respectively.

Figure 5 shows the variation of ln (I_0/I) as a function of C_Q for $[C_{14}C_4C_m\text{im}]Br_2$ and $[C_mC_4C_n\text{im}]Br_2$ series. The concentrations were all 2.0 mmol L^{-1} for the $[C_mC_4C_n\text{im}]Br_2$ series, and 1 mmol L^{-1} for the $[C_{14}C_4C_m\text{im}]Br_2$ ($m = 12, 14$) series. Each plot was fitted into a straight line and the slope was obtained. The N_{agg} values of $[C_{14}C_4C_{10}\text{im}]Br_2$, $[C_{14}C_4C_{12}\text{im}]Br_2$ and $[C_{14}C_4C_{14}\text{im}]Br_2$ were found to be 18, 20 and 22, respectively, implying that N_{agg} increased with increasing N_c for the disymmetric $[C_{14}C_4C_m\text{im}]Br_2$ series. For the disymmetric $[C_mC_4C_n\text{im}]Br_2$ series, N_{agg} were 16, 18, 21 and 27 for $m = 12$, 14, 16 and 18, respectively, as listed in Table 1. Obviously, the N_{agg} values were dependent on *m/n*, increasing from 16 to 27 as *m/n* increased from 1 to 3. The possible explanation was that the surfactant with the higher N_c or *m/n* can form a more compact micellar structure, because of the enhancement in the hydrophobic interaction. Such a trend of increasing N_{agg} values with increasing *m/n* has been found in the disymmetric $C_mC_6C_nBr_2$. However, the opposite relationship of decreasing N_{agg} values with increasing N_c or *m/n* was observed in the disymmetric $C_mC_3C_{14}PB$ or $C_mC_3C_nPB$, and this might result from the formation of premicelles. The more premicelles that could be formed, the lower the N_{agg}.

Acknowledgments We are grateful for the financial support from the Six Talent Peaks Program of Jiangsu Province, China (Project No. JNHB-001).

References

1. Song LD, Rosen MJ (1996) Surface properties, micellization, and premicellar aggregation of Gemini surfactants with rigid and flexible spacers. Langmuir 12:1149–1153
2. Zana R (2002) Dimeric and oligomeric surfactants, behavior at interfaces and in aqueous solution: a review. Adv Colloid Interface Sci 97:205–253
3. Chevalier Y (2002) New surfactants: new chemical functions and molecular architectures. Curr Opin Colloid Interface Sci 7:3–11
4. Zhong X, Guo JW, Feng LJ (2014) Cationic Gemini surfactants based on adamantane: synthesis, surface activity and aggregation properties. Colloids and Surfaces A 441:572–580
5. Zheng O, Zhao JX (2006) Solubilization of pyrene in the aqueous micellar solutions of Gemini surfactant C_{12}-s-C_{12}·2Br. J Colloid Interface Sci 300:749–754
6. Lu T, Lan Y, Liu C, Huang J, Wang Y (2012) Surface properties, aggregation behavior and micellization thermodynamics of a class of Gemini surfactants with ethyl ammonium head groups. J Colloid Interface Sci 377:222–230
7. Ding YS, Zha M, Zhang J, Wang SS (2007) Synthesis of a kind of geminal imidazolium ionic liquid with long aliphatic chains. Chin Chem Lett 18:48–50
8. Tookazu Y, Miri B, Keisuke M (2009) Surface properties and aggregate morphology of partially fluorinated carboxylate-type anionic gemini surfactants. J Colloid Interface Sci 339:230–235
9. Zhou LM, Chen H, Jiang XH, Lu F, Zhou YF (2009) Modification of montmorillonite surfaces using a novel class of cationic gemini surfactants. J Colloid Interface Sci 332:16–21
10. Song CP, Wu DQ, Zhang F, Liu P, Lu QH, Feng XL (2012) Gemini surfactant assisted synthesis of two-dimensional metalnanoparticles/graphene composites. Chem Commun 48:2119–2121
11. Zhou Y, Cheng Y, Han CY, Lai JL, Sui L, Luo GX (2014) Synthesis and surface properties of anionic Gemini surfactants having N-acylamide and carboxylate groups. J Surfact Deterg 17:727–732
12. Jain T, Tehrani-Bagha AR, Shekhar H, Crawford R, Johnson E, Norgaard K (2014) Anisotropic growth of gold nanoparticles using cationic gemini surfactants: effects of structure variations in head and tail groups. J Mater Chem C 2:994–1003
13. Sharma VD, Lees J, Hoffman NE, Brailoiu E, Madesh M, Wunder SL, Ilies MA (2014) Modulation of pyridinium cationic lipid–DNA complex properties by pyridinium Gemini surfactants and its impact on lipoplex transfection properties. Mol Pharmaceutics 11:545–559
14. Alami E, Beinert G, Marie P, Zana R (1993) Alkanediyl-.alpha., omega.-bis(dimethylalkylammonium bromide) Surfactants. 3. Behaviour at the Air-Water Interface. Langmuir 9:1465–1467
15. Silva SMC, Sousa JJS, Marques EF, Pais AACC, Michniak-Kohn BB (2013) Structure activity relationships in alkylammonium

C_{12}-Gemini surfactants used as dermal permeation enhancers. AAPS J 15:1119–1127
16. Zhou L, Jiang X, Li Y, Chen Z, Hu X (2007) Synthesis and properties of a novel class of Gemini pyridinium surfactants. Langmuir 23:11404–11408
17. Ao MQ, Xu GY, Zhu YY, Bai Y (2008) Synthesis and properties of ionic liquid-type Gemini imidazolium surfactants. J Colloid Interface Sci 326:490–495
18. Liu GY, Gu DM, Liu HY, Ding W, Li Z (2011) Enthalpy-entropy compensation of ionic liquid-type Gemini imidazolium surfactants in aqueous solutions: a free energy perturbation study. J Colloid Interface Sci 358:521–526
19. Jiang Z, Li X, Yang G, Cheng L, Cai B, Yang Y, Dong J (2012) pH-responsive surface activity and solubilization with novel pyrrolidone-based Gemini surfactants. Langmuir 28:7174–7181
20. Cai B, Dong JF, Cheng L, Jiang Z, Yang Y, Li XF (2013) Adsorption and micellization of gemini surfactants with pyrrolidinium head groups: effect of the spacer length. Soft Matter 9:7637–7643
21. Cai B, Li XF, Yang Y, Dong JF (2012) Surface properties of Gemini surfactants with pyrrolidinium head groups. J Colloid Interface Sci 370:111–116
22. Ao MQ, Huang PP, Xu GY, Yang XD, Wang YJ (2009) Aggregation and thermodynamic properties of ionic liquid-type gemini imidazolium surfactants with different spacer length. Colloid Polym Sci 287:395–402
23. Ao MQ, Xu GY, Pang JY, Zhao TT (2009) Comparison of aggregation behaviors between ionic liquid-type imidazolium Gemini surfactant [C12-4-C12im]Br 2 and its monomer [C12mim]Br on silicon wafer. Langmuir 25:9721–9727
24. Ren CC, Wang F, Zhang ZQ, Nie HH, Li N, Cui M (2015) Synthesis, surface activity and aggregation behavior of Gemini imidazolium surfactants 1,3-bis(3-alkylimidazolium-1-yl) propane bromide. Colloids Surf A 467:1–8
25. Antonietti M, Kuang DB, Smarsly B, Zhou Y (2004) Ionic liquids for the convenient synthesis of functional nanoparticles and other inorganic nanostructures. Chem Int Ed 43:4988–4992
26. Paul BK, Motra R (2005) Water solubilization capacity of mixed reverse micelles: effect of surfactant component, the nature of the oil, and electrolyte concentration. J Colloid Interface Sci 288:261–279
27. Leodidis EB, Hatton TA (1990) Amino acids in AOT reversed micelles. 1. Determination of interfacial partition coefficients using the phase-transfer method. J Phys Chem 94:6400–6411
28. Fry AJ (2003) Strong ion-pairing effects in a room temperature ionic liquid. J Electroanal Chem 546:35–39
29. Bai GY, Wang JB, Wang YJ, Yan HK (2002) Thermodynamics of hydrophobic interaction of disymmetric Gemini surfactants in aqueous solutions. J Phys Chem B 106:6614–6616
30. AIami E, HoImberg K, Eastoe J (2002) Adsorption properties of novel Gemini surfactants with nonidentical head groups. J Colloid Interface Sci 247:447–455
31. Peresypkin AV, Menger FM (1999) Zwitterionic geminis, coacervate formation from a single organic compound. Org Lett 1:1347–1350
32. Menger FM, Peresypkin AV (2001) A combinatorially-derived structural phase diagram for 42 zwitterionic geminis. J Am Chem Soc 123:5614–5615
33. Menger FM, Peresypkin AV (2003) Strings of vesicles: flow behavior in an unusual type of aqueous gel. J Am Chem Soc 125:5340–5345
34. Wang XY, Wang JB, Wang YL (2003) Micellization of a series of disymmetric Gemini surfactants in aqueous solution. J Phys Chem B 107:11428–11432
35. Sikirić M, Primožič I, Filipović-Vincekovic N (2002) Adsorption and association in aqueous solutions of disymmetric Gemini surfactant. J Colloid Interface Sci 250:221–229
36. Zou M, Dong JF, Yang GF, Li XF (2015) A comprehensive study on micellization of disymmetric pyrrolidinium headgroup-based gemini surfactants. Phys Chem Chem Phys 17:10265–10273
37. Kamboj R, Singh S, Chauhan V (2014) Synthesis, characterization and surface properties of *N*-(2-hydroxyalkyl)-*N*′-(2-hydroxyethyl) imidazolium surfactants. Colloids and Surfaces A 441:233–241
38. Wettig SD, Verrall RE (2001) Thermodynamic studies of aqueous m-s-m Gemini surfactant systems. J Colloid Interface Sci 235:310–316
39. Dong B, Li N, Zheng LQ, Inoue T (2007) Surface adsorption and micelle formation of surface active ionic liquids in aqueous solution. Langmuir 23:4178–4182
40. Dong B, Zhao XY, Zheng LQ, Zhang J, Li N, Inoue T (2008) Aggregation behavior of long-chain imidazolium ionic liquids in aqueous solution: micellization and characterization of micelle microenvironment. Colloids Surf A 317:666–672
41. Wang XD, Li QT, Chen X, Li ZH (2012) Effects of structure disymmetry on aggregation behaviors of quaternary ammonium Gemini surfactants in a protic ionic liquid EAN. Langmuir 28:16547–16554
42. Ruiz CC, Díaz-López L, Aguiar J (2007) Self-assembly of tetradecyltrimethylammonium bromide in glycerol aqueous mixtures: a thermodynamic and structural study. J Colloid Interface Sci 305:293–300
43. Tan JL, Zhao PJ, Ma DP, Feng SY, Zhang CQ (2013) Effect of hydrophobic chains on the aggregation behavior of cationic silicone surfactants in aqueous solution. Colloid Polym Sci 291:1487–1494
44. Fan YR, Li YJ, Cao MW, Wang JB, Wang YL, Thomas RK (2007) Micellization of disymmetric cationic Gemini surfactants and their interaction with dimyristoylphosphatidylcholine vesicles. Langmuir 23:11458–11464
45. Keyes-Baig C, Duhamel J, Wetting S (2011) Characterization of the behavior of a pyrene substituted Gemini surfactant in water by fluorescence. Langmuir 27:3361–3371
46. Wang XQ, Liu J, Yu L, Jiao JJ, Wang R, Sun LM (2013) Surface adsorption and micelle formation of imidazolium-based zwitterionic surface active ionic liquids in aqueous solution. J Colloid Interface Sci 391:103–110

Xiaohui Zhao is a doctoral candidate of applied chemistry at Nanjing University of Science and Technology, P. R. China. Her current research involves the synthesis and properties of Gemini imidazolium surfactants.

Dong An is a doctoral candidate of applied chemistry at Nanjing University of Science and Technology. His research involves the design, synthesis and performance of sugar esters nonionic surfactants.

Zhiwen Ye is a professor of School of Chemical Engineering at Nanjing University of Science and Technology. He is engaged in research on the synthesis, properties and application of surfactants.